

<sup>5</sup> Evans, J. W., "Development of Gun Probe Payloads and a 1750 Mc/s Telemetry System," MR-1749, AD 637 747, May 1966, Ballistic Research Labs., Aberdeen Proving Ground, Md.

<sup>6</sup> Marks, S. T., Pilcher, J. O., and Brandon, F. J., "The Development of a High Acceleration Testing Technique for the Electronic Instrumentation of HARP Projectile Systems," MR-1738, AD 635 782, March 1966, Ballistic Research Labs, Aberdeen Proving Ground, Md.

<sup>7</sup> Caudill, G. H., Taylor, B. C., and Melani, G., "The Development of an Improved Electric Detonator," MR-1684, AD 477 112, August 1965, Ballistic Research Labs., Aberdeen Proving Ground, Md.

<sup>8</sup> Boyer, E. D. and MacAllister, L. C., "Seven-Inch HARP Gun-Launched Vertical Probe System: Initial Development," MR-1770, AD 640 825, July 1966, Ballistic Research Labs., Aberdeen Proving Ground, Md.

<sup>9</sup> Mermagen, W. H., "Measurements of the Dynamical Behavior of Projectiles Over Long Flight Paths," AIAA Paper 70-538, Tullahoma, Tenn., May 1970.

## Attitude Motion in an Eccentric Orbit

D. K. ANAND,\* R. S. YUHASZ,† J. M. WHISNANT‡  
*Johns Hopkins University, Applied Physics  
 Laboratory, Silver Spring, Md.*

### I. Introduction

IN a previous paper<sup>1</sup> the capture and stability of a gravity-gradient satellite in an eccentric orbit was reported. A stroboscopic<sup>2</sup> study of the motion at apogee was conducted and it was shown that the satellite could be captured by magnetically steering the satellite into the stable region. This note reports the results of further stroboscopic as well as analytical studies of the oscillations and stability regions of a gravity-gradient satellite in an eccentric orbit.

### II. Analysis

Satellite oscillations in the plane of an elliptic orbit are described by<sup>3,4</sup>

$$(1 + e \cos \nu)(d^2 \varphi / d\nu^2) - 2e \sin \nu (d\varphi / d\nu) + \omega^2 \sin \varphi \cos \varphi = 2e \sin \nu \quad (1)$$

where  $e$  is the orbital eccentricity,  $\omega^2 = 3[(I_x - I_z)/I_y]$ ,  $\varphi$  is the pitch libration angle measured from the local vertical,  $\nu$  is the true anomaly and  $I_x, I_y, I_z$  are the principle moments

Received February 10, 1971; revision received May 3, 1971. This work was done under U.S. Navy Contract N00017-62-C-0604 and supported by the Naval Air Systems Command. The authors thank Martins Sturmanis for doing the programming involved in this study.

\* Senior Staff, Space Research and Analysis Branch; also Associate Professor of Mechanical Engineering, University of Maryland.

† Associate Physicist, Space Research and Analysis Branch.

‡ Mathematician, Space Research and Analysis Branch.

of inertia. This equation has been investigated by researchers using both numerical integration and phase space representations. Here we consider a perturbational technique.

The term  $\sin \varphi \cos \varphi$  in Eq. 1 may be expanded in a MacLaurin series so that the pitch equation becomes

$$(d^2 \varphi / d\nu^2) + \omega^2 \varphi = 2e \sin \nu + 2(d\varphi / d\nu)e \sin \nu - (d^2 \varphi / d\nu^2)e \cos \nu + \frac{2}{3}\omega^2 \varphi^3 + \dots \quad (2)$$

If the  $\varphi^3$  and higher order terms are neglected then the second-order approximation to Eq. (2) is amenable to an analytic asymptotic treatment described by Struble.<sup>5</sup>

It is assumed that the solution can be expressed as a series expansion in terms of the small parameter  $e$ ,

$$\varphi = A_0 \cos(\omega \nu - \theta) + A_1 e + A_2 e^2 + A_3 e^3 + \dots \quad (3)$$

where  $A_0, \theta, A_1, A_2, A_3$  are treated as variables. The technique combines the use of variation of parameters as well as a perturbation method with the expansion in terms of  $e$ .

The process begins by substituting Eq. (3) into the approximation to Eq. (2) and equating like powers of eccentricity. This yields

$$[\ddot{A}_0 - A_0(\omega - \dot{\theta})^2 + \omega^2 A_0] \cos(\omega \nu - \theta) = 0 \quad (4a)$$

$$[A_0 \ddot{\theta} - 2\dot{A}_0(\omega - \dot{\theta})] \sin(\omega \nu - \theta) = 0 \quad (4b)$$

$$\ddot{A}_1 + \omega^2 A_1 = 2[\dot{A}_0 \cos(\omega \nu - \theta) + 1 -$$

$$A_0(\omega - \dot{\theta}) \sin(\omega \nu - \theta)] \sin \nu -$$

$$[\ddot{A}_0 - A_0(\omega - \dot{\theta})^2] \cos(\omega \nu - \theta) \cos \nu -$$

$$[A_0 \ddot{\theta} - 2\dot{A}_0(\omega - \dot{\theta})] \sin(\omega \nu - \theta) \cos \nu \quad (4c)$$

$$\ddot{A}_2 + \omega^2 A_2 = 2 \sin \nu \dot{A}_1 - \ddot{A}_1 \cos \nu \quad (4d)$$

Since  $A_0$  and  $\theta$  determine the solution for zero eccentricity, they are treated as constants in Eq. (4c). This allows us to solve for  $A_1$  which yields the solution to first order in eccentricity. Now we substitute the results in Eq. (3) and back in Eq. (2) and obtain a new set of variational equations similar to Eqs. (4a) and (4b) which are now complete to second order. The solution to these equations tells us that  $A_0$  can be considered constant to second order (in eccentricity) but that  $\theta$  varies as  $e^2 \nu$ . The solution to Eq. (4d) can then be

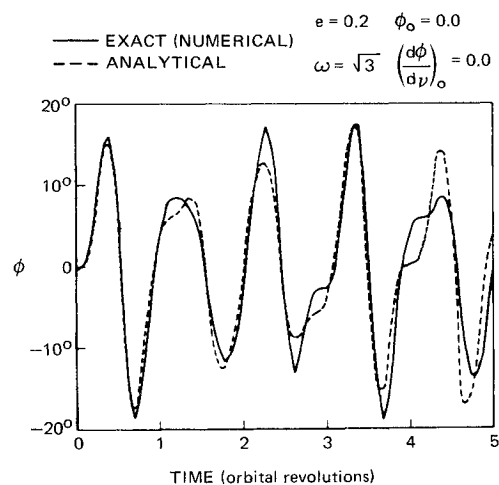


Fig. 1 Comparison of analytical and numerical solutions of Eq. (1).

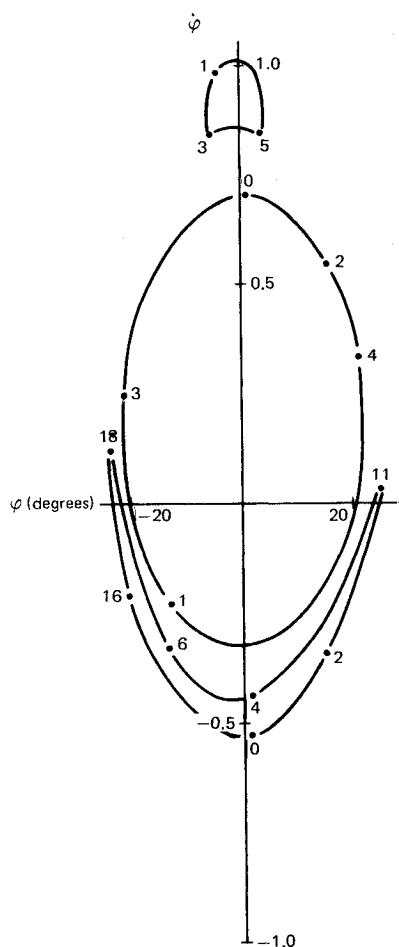


Fig. 2a Stable regions at  $\nu = 0$  for  $e = 0.2$ ,  $\omega^2 = 3$ .

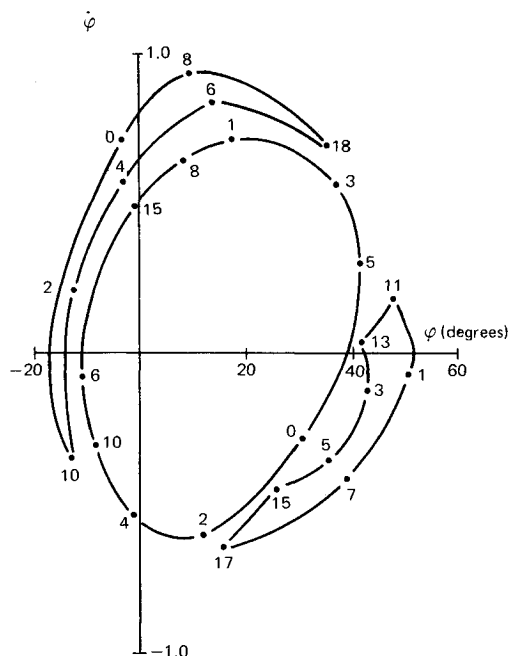


Fig. 2b) Stable regions at  $\nu = \pi/2$  for  $e = 0.2$ ,  $\omega^2 = 3$ .

obtained. Substituting  $A_2$  into Eq. (3) and then into Eq. (2) allows us to increase the order of the solution. The solution, correct to second order in  $e$ , is:

$$A_0 = \text{constant} \quad (5a)$$

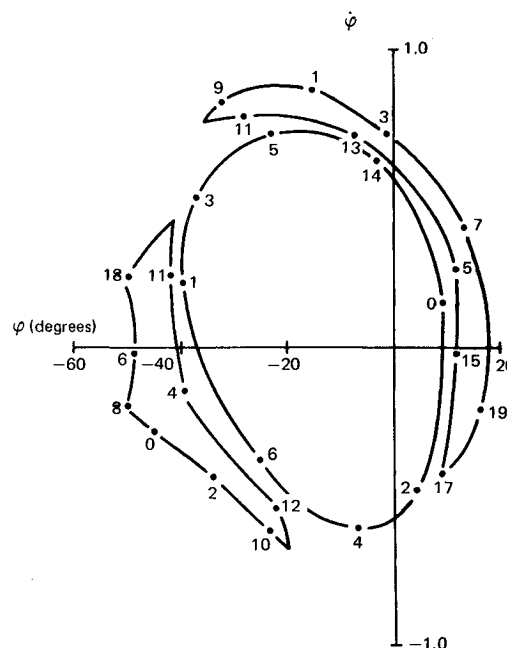


Fig. 2c Stable regions at  $\nu = 3\pi/2$  for  $e = 0.2$ ,  $\omega^2 = 3$ .

$$\theta = \theta_0 - [3e^2\nu\omega(\omega^2 - 1)]/[4(4\omega^2 - 1)] \quad (5b)$$

$$A_1 = 2 \sin\nu/(\omega^2 - 1) + [(\omega - 2)B_1^- - (\omega + 2)B_1^+]A_0\omega/2 \quad (5c)$$

$$A_2 = 3 \sin 2\nu/[(\omega^2 - 1)(\omega^2 - 4)] + [(\omega - 2)(\omega - 3)B_2^- + (\omega + 2)(\omega + 3)B_2^+]A_0\omega/16 \quad (5d)$$

where

$$B_j^\pm = \cos[(\omega \pm j)\nu - \theta]/(2\omega \pm 1)$$

The pitch angle  $\varphi$  obtained from the above equation for  $e = 0.2$  and  $\omega^2 = 3$  is compared in Fig. 1 to the value of  $\varphi$  obtained by numerically integrating Eq. (1). The two solutions are seen to agree both in phase and magnitude. It is noted that the agreement obtained is substantially the same as the WKBJ approximation<sup>6</sup> to Eq. (1). However, when  $\varphi$  gets larger the agreement is not sufficient for constructing stability charts, although this analytical technique has been used for determining regions of resonance.<sup>7</sup>

For further studies the complete nonlinear equations of attitude motion were developed using the Lagrangian approach.<sup>1</sup> External forces that arise from the gravitational, magnetic, and solar environments were included in the formulation. The solar effect consists of both thermal distortion of the stabilizing booms and a radiation pressure torque on the deformed spacecraft. The magnetic torques are represented by a geomagnetic field model written in terms of spherical harmonics. An analytical model for hysteretic damping was developed and included. The equations were numerically integrated and it was established that for practical stability the satellite librations should be bounded for 75 orbits. The resulting stability charts, constructed using the stroboscopic techniques, are shown in Fig. 2. It is noted that the regions of stability obtained are larger than those reported in earlier works<sup>3,4</sup> where external forces were not included. A large stability region facilitates the capture, by magnetic maneuvering, since  $\dot{\varphi} = -1$  is out of the stable region for certain combinations of eccentricity and true anomaly.

## References

- <sup>1</sup> Anand, D. K., Whisnant, J. M., Pisacane, V. L., and Sturmanis, M., "Gravity-Gradient Capture and Stability in an Eccentric Orbit," *Journal of Spacecraft and Rockets*, Vol. 6, No. 12, Dec. 1969, pp. 1456-1459.
- <sup>2</sup> Minorsky, N., *Nonlinear Oscillations*, Van Nostrand, Princeton, N.J., 1962, Chap. 16, pp. 390-415.
- <sup>3</sup> Zlatoustov, U. A., Okhotsimsky, D. E., Sarychev, V. A., and Torzhevsky, A. P., "Investigation of Satellite Oscillations in the Plane of an Elliptic Orbit," *Proceedings of the 11th International Congress of Applied Mechanics*, Springer-Verlag, Berlin, 1966, pp. 436-439.
- <sup>4</sup> Brereton, R. C. and Modi, V. J., "On the Stability of Planar Librations of a Dumbbell Satellite in an Elliptic Orbit," *Journal of the Royal Aeronautical Society*, Vol. 70, No. 672, Dec. 1966, pp. 1098-1102.
- <sup>5</sup> Struble, R. A., *Nonlinear Differential Equations*, McGraw-Hill, New York, 1962.
- <sup>6</sup> Modi, V. J. and Brereton, R. C., "Libration Analysis of a Dumbbell Satellite Using the WKBJ Method," *Journal of Applied Mechanics*, Vol. 33, No. 3, Sept. 1966, pp. 676-678.
- <sup>7</sup> Beletsky, V. V., "The Libration of a Satellite on an Elliptic Orbit," *Dynamics of Satellites*, Academic Press, New York, 1963, pp. 219-230.

## Determination of Gravity at Apollo 14 Landing Site

JOSEPH ST. AMAND\* AND KENNETH R. GOODWIN JR.\*  
Charles Stark Draper Laboratory, Massachusetts Institute  
of Technology, Cambridge, Mass.

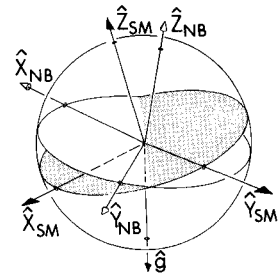
### Introduction

DURING the flight of Apollo 14, a measurement of the lunar gravitational field was made at the LM landing site (Fra Mauro). Due to electrical power constraints, the experiment was of short duration and did not interfere with the crew's preparations for the first extra vehicular activity (EVA) period. The measurement utilized the X-accelerometer of the LM Primary Guidance Navigation and Control System (PGNCS).<sup>1</sup> Essential to the experiment was a knowledge of the orientation of the LM navigation base (NB) with respect to the local gravity vector  $\mathbf{g}$ . This information was obtained from the Lunar Surface Alignment Program which preceded the experiment. This Note describes how the information was used to determine  $\mathbf{g}$  and how the value so obtained compares with the values obtained from four lunar gravity models.

### Equipment

The apparatus employed to measure  $\mathbf{g}$  consisted of two standard pieces of Apollo equipment: the LM Inertial Measurement Unit (IMU), and the LM Guidance Computer (LGC).<sup>1</sup> The IMU is a gimbaled, three degree-of-freedom, gyroscopically stabilized device. Of interest here are two sets of coordinate axes associated with the IMU. The first is the LM NB with unit vectors  $\hat{\mathbf{X}}_{NB}$ ,  $\hat{\mathbf{Y}}_{NB}$ , and  $\hat{\mathbf{Z}}_{NB}$ . This

Fig. 1 Coordinate axes pertinent to the gravity experiment.



system is defined with respect to the LM structural body. The second coordinate system is that of the IMU Stable Member. This system is defined by the orientation of three orthogonally mounted accelerometers. Let  $\hat{\mathbf{X}}_{SM}$ ,  $\hat{\mathbf{Y}}_{SM}$ , and  $\hat{\mathbf{Z}}_{SM}$  represent the unit vectors of this coordinate system. The orientation of the NB with respect to the stable member is uniquely specified by three angles: outer gimbal angle (OGA); inner gimbal angle (IGA); middle gimbal angle (MGA).

More specifically, the sensor of the gravitational acceleration was a Pulsed Integrating Pendulum Accelerometer (PIPA).<sup>1</sup> The equation governing the output of a PIPA is

$$a_i = (1 + SFE_i)(\Delta N_i / \Delta T) - B_i \quad (1)$$

where:  $\Delta N_i$  = the number of pulses from the  $i$ th accelerometer during the time  $\Delta T$ ;  $B_i$  = the bias of the  $i$ th accelerometer (the acceleration indicated in a zero  $\mathbf{g}$  environment);  $SFE_i$  = scale factor error of the  $i$ th accelerometer†; and  $a_i$  = the average acceleration sensed by the  $i$ th accelerometer during the time  $\Delta T$ . Because the bias is acceleration history sensitive, the equipment was used in such a way that the uncertainty in the bias of the X-accelerometer was inconsequential.

### Methodology

After determining the orientation of the LM NB with respect to  $\mathbf{g}$ , the gimbal angles required to align the X-accelerometer parallel and antiparallel to  $\hat{\mathbf{g}}$  ( $\hat{\mathbf{g}} = \mathbf{g}/g$ ) were calculated. The geometry of the problem is as given in Fig. 1. It can be shown that, given the orientation of  $-\hat{\mathbf{g}}$  with respect to the NB, the gimbal angles required to align  $\hat{\mathbf{X}}_{SM}$  parallel to  $\hat{\mathbf{g}}$  (position one) are given by:

$$OGA_1 = 0.00^\circ \quad (2a)$$

$$IGA_1 = +\sin^{-1}\gamma + 180.00^\circ \quad (2b)$$

$$MGA_1 = -\sin^{-1}(\beta / \cos IGA) \quad (2c)$$

To position  $\hat{\mathbf{X}}_{SM}$  antiparallel to  $\hat{\mathbf{g}}$  (position two),  $OGA_2 = OGA_1$ ,  $MGA_2 = MGA_1$  and the inner gimbal angle is given by

$$IGA_2 = +\sin^{-1}\gamma \quad (3)$$

Here  $\beta$  and  $\gamma$  are the components of  $-\hat{\mathbf{g}}$  along  $\hat{\mathbf{Y}}_{NB}$  and  $\hat{\mathbf{Z}}_{NB}$ , respectively.

The values of  $\beta$  and  $\gamma$  were obtained via telemetry during the alignment program. Then, teams at the Manned Spacecraft Center (MSC) and the Draper Laboratory used Eqs. (2) and (3) to determine the required gimbal angles. While the crew was engaged in EVA I preparation, the IMU was aligned

† To convert the number of pulses from an accelerometer into a mean acceleration,  $\Delta N_i / \Delta T$  is ideally multiplied by a scale factor ( $SF$ ) of 1 cm/sec/pulse. However, in practice the true scale factor is not unity and is instead given by  $SF = (1 + SFE)$  cm/sec/pulse, where  $SFE$  is a small correction expressed in parts per million (ppm).